TRANSMITTED WAVES AND THE DYNAMIC EDGE EFFECT IN AN ANISOTROPIC STRIP. (COMPARISON WITH EXPERIMENTAL DATA)

A. G. Demeshkin and V. M. Kornev

UDC 678.067.001

The refined problem of the spreading of steady-state boundary operating conditions in an orthotropic strip is solved. The refinement in this problem involves allowance for the shear and compression in the orthotropic layer. The theoretical estimates obtained for the zone of penetration of the edge effect are compared qualitatively with the results of experiments performed on composite rods.

1. Analysis of Longitudinal Vibrations of an Anisotropic Strip. Consider the equations of the dynamics of an elastic orthotropic strip in the case of two-dimensional strain [1, 2],

$$\frac{E_1}{1-\nu_1\nu_2}\left(\frac{\partial^2 U}{\partial x^2}-\nu_2\frac{\partial^2 W}{\partial x\,\partial y}\right)+G\left(\frac{\partial^2 U}{\partial y^2}+\frac{\partial^2 W}{\partial x\,\partial y}\right)=\rho c^2\frac{\partial^2 U}{\partial t^2},$$
$$G\left(\frac{\partial^2 U}{\partial x\,\partial y}+\frac{\partial^2 W}{\partial x^2}\right)-\frac{E_2}{1-\nu_1\nu_2}\left(\nu_1\frac{\partial^2 U}{\partial x\,\partial y}+\frac{\partial^2 W}{\partial y^2}\right)=\rho c^2\frac{\partial^2 W}{\partial t^2} \qquad (1.1)$$

with the following boundary conditions at the side surfaces of the strip and at the end-face:

$$\sigma_y=0,\ \tau=0 \quad \text{for } y=-1;\ 1,$$
$$\sigma_x=\sigma^0(y,\ t),\ \tau=\tau^0(y,\ t) \quad \text{for } x=0, \qquad (1.2)$$

while the stresses σ_x, σ_y, and τ are calculated by means of the expressions given in [3]. Here, U and W are the displacements along and across the layer; E_1, E_2, and G are the elasticity moduli; ν_1 and ν_2 are the Poisson brackets; ρ is the reduced density of the material, and $c=[E_1/\rho(1-\nu_1\nu_2)]^{1/2}$ is the reduced rate of disturbance propagation in the direction of the x axis. The measurement units are the following: 2h is the plate thickness, τ is the time during which a perturbation at the x = 0 section traverses a distance equal to h: $t_1 = tc/h$, $x_1 = x/h$, and $y_1 = y/h$. The subscript 1 will be subsequently omitted.

We shall reduce the problem (1.1), (1.2) to a one-dimensional problem. We expand the displacements U and W in series with respect to Legendre polynomials $P_i(y)$ [2]. We multiply the equations of system (1.1) and the boundary conditions (1.2) by the Legendre polynomials and perform integration along the plate thickness. In performing integration by parts of relationships (1.1), we use the conditions at the side surfaces (1.2). Using the well-known relationships for Legendre polynomials, we obtain two infinite systems of equations (for an isotropic material, similar systems are given in [1], the first of which corresponds to the problem of longitudinal vibrations, while the second pertains to the problem of flexural vibrations of the strip). We shall consider only the problem involving longitudinal vibrations for steady-state boundary operating conditions. In the expansion

$$U=\sum_{i=1}^{\infty}\frac{2i+1}{2}U_i(x,\ t)\,P_i(y),\quad W=\sum_{i=1}^{\infty}\frac{2i+1}{2}W_i(x,\ t)\,P_i(y) \qquad (1.3)$$

we retain the approximation which accounts only for the functions U_0, W_1, and U_2. In our case, the system of equations for longtitudinal vibrations of the strip assumes the following form:

Novosibirsk. Translated from Zhurnal Prikladnoi Mekhaniki i Tekhnicheskoi Fiziki, No. 2, pp. 144-149, March-April, 1991. Original article submitted November 2, 1989.

0021-8944/91/3202-0274$12.50

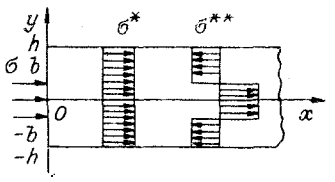

Fig. 1

$$\frac{\partial^2 U_0}{\partial x^2} + 3\nu_2 \frac{\partial W_1}{\partial x} - \frac{\partial^2 U_0}{\partial t^2} = 0,$$

$$a_{21} \frac{\partial U_0}{\partial x} - \delta^2 \frac{\partial^2 W_1}{\partial x^2} - W_1 + a_{23} \frac{\partial U_2}{\partial x} - \alpha_1^2 \frac{\partial^2 W_1}{\partial t^2} = 0, \tag{1.4}$$

$$a_{32} \frac{\partial W_1}{\partial x} + \varepsilon^2 \frac{\partial^2 U_2}{\partial x^2} - U_2 + \alpha_2^2 \frac{\partial^2 W_2}{\partial t^2} = 0,$$

where $a_{21} = -\nu_1/3$; $a_{23} = 5G(1 - \nu_1\nu_2)/3E_2$; $a_{32} = -1/5$; $\delta^2 = G(1 - \nu_1\nu_2)/3E_2$; $\varepsilon^2 = E_1/15G \times (1 - \nu_1\nu_2)$; $\alpha_1^2 = E_1/3E_2$; $\alpha_2^2 = E_1/15G(1 - \nu_1\nu_2)$. The boundary conditions for system (1.4) are

$$\frac{\partial U_0}{\partial x} + 3\nu_2 W_1 = \int_{-1}^{1} \sigma^0(y, t) P_0(y)\, dy,$$

$$\frac{\partial W_1}{\partial x} + 5U_2 = \int_{-1}^{1} \tau^0(y, t) P_2(y)\, dy, \quad \frac{\partial U_2}{\partial x} = \int_{-1}^{1} \sigma^0(y, t) P_2(y)\, dy. \tag{1.5}$$

For solving system (1.4), we introduce a resolving function V(x, y), such that

$$U_0 = 3\nu_2 \frac{\partial V}{\partial x}, \quad W_1 = \frac{\partial^2 V}{\partial t^2} - \frac{\partial^2 V}{\partial x^2},$$

$$\frac{\partial U_2}{\partial x} = \frac{1}{a_{23}} \left[\alpha_1^2 \frac{\partial^4 V}{\partial t^4} - (\delta^2 + \alpha_1^2) \frac{\partial^4 V}{\partial x^2 \partial t^2} + \frac{\partial^2 V}{\partial t^2} - \frac{\partial^2 V}{\partial x^2} + \delta^2 \frac{\partial^4 V}{\partial x^4} - 3\nu_2 a_{21} \frac{\partial^2 V}{\partial x^2} \right]. \tag{1.6}$$

Then, the first and the second equations of system (1.4) are satisfied identically, while the third one yields for the resolving function V(x, t) the equation

$$\left[a_{23} a_{32} \frac{\partial^2}{\partial x^2} \left(\frac{\partial^2}{\partial x^2} - \frac{\partial^2}{\partial t^2} \right) + 3\nu_2 a_{21} \frac{\partial^2}{\partial x^2} \left(\varepsilon^2 \frac{\partial^2}{\partial x^2} - 1 - \alpha_2^2 \frac{\partial^2}{\partial t^2} \right) - \right.$$

$$\left. - \left(\frac{\partial^2}{\partial x^2} - \frac{\partial^2}{\partial t^2} \right) \left(\varepsilon^2 \frac{\partial^2}{\partial x^2} - 1 - \alpha_2^2 \frac{\partial^2}{\partial t^2} \right) \left(\delta^2 \frac{\partial^2}{\partial x^2} - 1 - \alpha_1^2 \frac{\partial^2}{\partial t^2} \right) \right] V = 0. \tag{1.7}$$

For steady-state excitation of vibrations, we shall seek the solution for the resolving function V(x, t) in the following form:

$$V(x, t) = A \exp\{i(\omega_1 t - kx)\}, \tag{1.8}$$

where $\omega_1 = \omega h/c$ is the dimensionless frequency, and h is the half-width of the strip. The subscript 1 will subsequently be omitted. By substituting (1.8) in (1.7), we obtain the bicubic equation

$$(k^2 - \omega^2)(\varepsilon^2 k^2 + 1 - \alpha_2^2 \omega^2)(\delta^2 k^2 + 1 - \alpha_1^2 \omega^2) +$$

$$+ 3\nu_2 a_{21} k^2 (\varepsilon^2 k^2 + 1 - \alpha_2^2 \omega^2) + a_{23} a_{32} k^2 (k^2 - \omega^2) = 0. \tag{1.9}$$

TABLE 1

Specimen No.	d	D	L	l_1	l_2	E_C	E_1	E_2	G	χ, %	ν_1	ν_2	ρ, g/cm^3	ω^2	ε_1	δ_1	$\frac{E_1}{G}$	$\frac{q_0}{D}$	$\frac{q_1}{D}$	$\frac{q_\infty}{D}$
	mm					MPa														
1	3	20	400	500	480	700	4 700	850	260	2	0,4	0.072	1,36	0,03	1,12	0,3	18,0	4,2	4,4	6
2	3	20	400	500	480	2400	7 150	2920	880	2	0,4	0,163	1,36	0,02	0,76	0,3	8,1	2,7	2,9	5,6
3	6	12	400	500	480	2700	56 000	4000	1180	20	0,4	0,03	2,52	0,002	1,79	0,3	47,5	7,3	7,5	12
4	3	30	400	500	400	2600	5 100	3200	940	1	0,4	0,25	1,3	0,05	0,63	0,3	5,4	1,7	2,5	4
5	6	20	400	500	400	2600	18 000	3400	1000	8	0,4	0,073	1,7	0,01	1,13	0,3	18,6	4,2	4,4	6

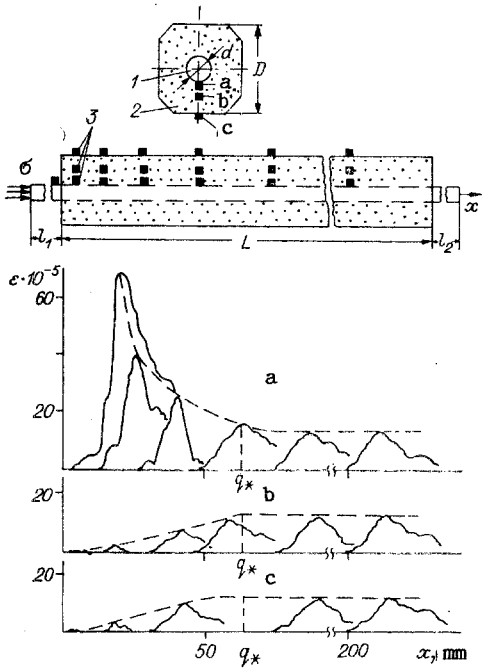

Fig. 2

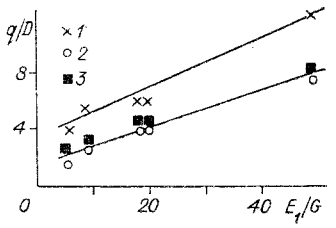

Fig. 3

By solving (1.9), we find the roots $k_{1,2} = \pm\gamma_1$, $k_{3,4} = \pm\gamma_2$, and $k_{5,6} = \pm\gamma_3$. Then, the expression for the resolving function V(x, t) for a wave propagating to the right (x > 0) is written thus:

$$V(x, t) = \sum_{n=1}^{3} A_n \exp[i(\omega t - \gamma_n x)]. \tag{1.10}$$

The amplitudes A_n for steady-state boundary operating conditions at x = 0 are determined from boundary conditions (1.5).

The procedure for determining the roots of the bicubic equation and subsequent analysis are simplified considerably if we put in the system of equations (1.4) the coefficients $a_{21} = a_{32} = 0$, whose absolute values are smaller than unity. By omitting terms with the coefficients a_{21} and a_{32} in front of the lowest derivatives, we do not change the type of Eq. (1.7); the solution obtained for the functions U_0, W_1, and U_2 differs from the complete solution (1.6) by the terms with small parameters of the order of $|a_{21}|$ and $|a_{32}|$. In comparing the experimental and theoretical results, we shall perform below numerical calculations of U(x, t) with and without an allowance for the coefficients a_{21} and a_{32}.

Thus, putting $a_{21} = a_{32} = 0$ in Eq. (1.9), we find

$$(k^2 - \omega^2)(\varepsilon^2 k^2 + 1 - \alpha_2^2\omega^2)(\delta^2 k^2 + 1 - \alpha_1^2\omega^2) = 0,$$

whence we immediately determine the roots of the equation

$$k_{1,2} = \pm\omega,\ k_{3,4} = \pm\delta^{-1}(\alpha_1^2\omega^2 - 1)^{1/2},$$
$$k_{5,6} = \pm\varepsilon^{-1}(\alpha_2^2\omega^2 - 1)^{1/2}.$$

The solution for the resolving function V(x, t) is given by

$$V(x, t) = A_1 \exp[-i\omega(t - x)] + A_2 \exp[i\omega t - x(1 - \alpha_1^2\omega^2)^{1/2}/\delta] +$$
$$+ A_3 \exp[i\omega t - x(1 - \alpha_2^2\omega^2)^{1/2}/\varepsilon].$$

The character of the solution can change, and different variants may arise, with variation of the frequency parameter ω. We shall only consider the case where $\alpha_1^2\omega^2 < 1$ and $\alpha_2^2\omega^2 < 1$ (the other cases, $\alpha_1^2\omega^2 > 1$, $\alpha_2^2\omega^2 > 1$; $\alpha_1^2\omega^2 < 1$, $\alpha_2^2\omega^2 > 1$ ... are analyzed in a similar way):

$$U_0(x,t) = iA_{11}\exp[i\omega(t-x)] + A_{12}\exp\left[i\omega t - x\delta^{-1}(1-\alpha_1^2\omega^2)\right] + A_{13}\exp\left[i\omega t - x\varepsilon^{-1}(1-\alpha_2^2\omega^2)\right],$$
$$W_1(x,t) = A_{22}\exp\left[i\omega t - x\delta^{-1}(1-\alpha_1^2\omega^2)\right] + A_{23}\exp\left[i\omega t - x\varepsilon^{-1}(1-\alpha_2^2\omega^2)\right], \quad (1.11)$$
$$U_2(x,t) = A_{33}\exp\left[i\omega t - x\varepsilon^{-1}(1-\alpha_1^2\omega^2)\right].$$

Here, the coefficients A_{ij} depend on the frequency ω. The solution for longitudinal vibrations was obtained in the form of three components: the solution of the transmitted-wave type with the amplitude A_{11} and solutions of the two edge effects, which are localized near the end-face to which the load is applied. The zone of penetration of the dynamic edge effect is determined by the parameters δ and ε. The smaller these parameters and the frequency, the closer to the strip's end-face the edge effect occurs, and vice versa.

We shall now consider an anisotropic strip, to the end-face of which (x = 0) a steady-state dynamic load is applied over a section whose width is equal to 2b (Fig. 1). We decompose the load σ of unit intensity which acts at the end-face of the strip into two components: σ^*, which is uniformly distributed with the intensity β over the entire width of the strip, and the self-balancing load σ^{**}. Then, in the absence of shearing forces τ^0, with an allowance for the decomposition of the acting load σ into the two components σ^* and σ^{**}, the boundary conditions (1.4) assume the following form:

$$\frac{\partial U_0}{\partial x} + 3\nu_2 W_1 = \sigma_1, \quad \frac{\partial W_1}{\partial x} + 5U_2 = 0, \quad \frac{\partial U_2}{\partial x} = \sigma_2, \quad (1.12)$$

where

$$\sigma_1 = \int_{-1}^{1} \sigma^* P_0(y)\,dy; \quad \sigma_2 = \int_{-1}^{1} \sigma^{**} P_2(y)\,dy.$$

For determining the coefficients A_{ij} in Eqs. (1.11), we substitute the resolving function V(x, t) in (1.6) and (1.12). After certain transformations, we obtain the following expressions for A_{ij}:

$$A_{11} = 3\nu_2\left[\frac{\sigma_2}{3\nu_2\omega^2} - \frac{5\delta^3\sigma_2}{\omega^2\delta^2 + 1 - \alpha_1^2\omega^2}\left(\frac{\delta^2(1-\alpha_2^2\omega^2)^{1/2}}{\varepsilon^2\gamma(1-\alpha_1^2\omega^2)^{1/2}} + \frac{\varepsilon}{(1-\alpha_1^2\omega^2)^{1/2}(1-\alpha_2^2\omega^2)^{1/2}} - \frac{a_{23}\sigma_2}{\gamma}\right)\right],$$
$$A_{12} = -\frac{15\nu_2\delta^3\sigma_2}{\omega^2\delta^2 + 1 - \alpha_1^2\omega^2}\left[\frac{\delta^2(1-\alpha_2^2\omega^2)^{1/2}}{\varepsilon^2\gamma(1-\alpha_1^2\omega^2)^{1/2}} + \frac{\varepsilon}{(1-\alpha_1^2\omega^2)^{1/2}(1-\alpha_2^2\omega^2)^{1/2}}\right], \quad (1.13)$$
$$A_{13} = 3\nu_2 a_{23}\sigma_2(1-\alpha_2^2\omega^2)^{1/2}/\varepsilon\gamma,$$
$$A_{23} = a_{23}\sigma_2/\varepsilon^2\gamma, \quad A_{33} = \gamma\varepsilon/a_{23}(1-\alpha_2^2\omega^2)^{1/2}$$
$$\left(\gamma = \varepsilon^{-4}\left[\delta^2(1-\alpha_2^2\omega^2) - \varepsilon^2(1-\alpha_1^2\omega^2)\right]\right).$$

In the approximation under consideration, where only the functions U_0, W_1, and U_2 are taken into account, relationships (1.3) yield the following for longitudinal strip vibrations:

$$\tilde{U}(x, y, t) = 0{,}5\left[U_0(x, t)P_0(y) + 2{,}5U_2(x, t)P_2(y)\right]. \quad (1.14)$$

We substitute in (1.14) the expressions for the Legendre polynomials and the expressions for $U_0(x, t)$ and $U_2(x, t)$ from (1.11):

$$\tilde{U}(x, y, t) - 0{,}5A_{11}\sin\omega(t-x) = R(x, y)\exp(i\omega t),$$
$$R(x, y) = 0{,}5\left\{A_{12}\exp\left[-x\delta^{-1}(1-\alpha_1^2\omega^2)^{1/2}\right] + \left[A_{13} + 2{,}5(3y^2-1)\right]\times\exp\left[-x\varepsilon^{-1}(1-\alpha_2^2\omega^2)^{1/2}\right]\right\}. \quad (1.15)$$

The dynamic edge effect R(x, y) is determined by the right-hand side of relationship (1.15); it has exponential factors, which diminish the faster, the larger the values of δ^{-1} and ε^{-1} become, as x increases.

We introduce a zone of penetration of the dynamic edge effect q, such that

$$\alpha = R(q, y)/R(0, y),$$

$$\alpha = \frac{A_{12}\exp\left[-q\delta^{-1}\left(1-\alpha_1^2\omega^2\right)^{1/2}\right]}{A_{12}+A_{13}+2{,}5A_{33}\left(3y^2-1\right)}+ \qquad (1.16)$$

$$\frac{\left[A_{13}+2{,}5A_{33}\left(3y^2-1\right)\right]\exp\left[-q\varepsilon^{-1}\left(1-\alpha_2^2\omega^2\right)^{1/2}\right]}{A_{12}+A_{13}+2{,}5A_{33}\left(3y^2-1\right)}.$$

Outside this zone, the edge effect R(x, y) is negligibly small in comparison with R(0, y): In practical calculations, it was assumed that $\alpha = 0.05$, which was connected with the accuracy in measuring the dynamic processes.

For $\varepsilon \gg \delta$, the value of q is determined by the relationship

$$q = \varepsilon\left(\ln\alpha - \ln\zeta\right)/\left(1-\alpha_2^2\omega^2\right)^{1/2},$$

where

$$\zeta = \frac{A_{13}+2{,}5A_{33}\left(3y^2-1\right)}{A_{12}+A_{13}+2{,}5A_{33}\left(3y^2-1\right)}.$$

2. Qualitative Comparison between the Theoretical and Experimental Results. We shall compare the theoretical estimates obtained for the edge effect zone (1.6) with the results of experiments performed on composite rods [4]. The field of longitudinal strain in a monodirectional composite consisting of a steel rod and an epoxy binder was determined experimentally in [4]. A dynamic load was applied to the end-face of the steel rod. In addition to the published experimental results, we also performed a series of experiments differing from those in [4] by the method of load application to the specimen (a compression pulse was created in the steel rod) and by the arrangement of tensometric sensors, which were pasted at three levels over the cross section and the length of the composite. Figure 2 shows the arrangement of tensors over sections a-c and the typical oscillograms obtained from the tensometric sensors for one of the experiments performed (1, steel rod with the diameter d; 2, expoxy binder, 3, tensometric sensors). The experimental results indicate that the amplitude of the strain pulse in the steel rod decreases in moving away from the end-face, while it increases in the binder. Beginning with a certain distance $x = q_*$ from the end-face x = 0, a constant-amplitude pulse propagates along the composite (along both the steel rod and the binder). We shall refer to the quantity q_* as the experimental zone of penetration of the edge effect. Table 1 provides the geometric and rigidity characteristics of the composite rods and their components, as well as the measured zone of penetration of the edge effect q_*. It should be mentioned that we addressed ourselves to the problem of determining the variation of q_* over the cross section of the composite in the series of additional experiments, where the sensors were arranged in three sections. However, the scatter of experimental data and the spacing in the arrangement of the sensors did not make it possible to determine the character of this variation with a sufficient degree of accuracy.

The rule of mixtures [5] was used for determining the average values of the characteristics E_1, E_2, G, ν_1, and ν_2 of the specimens tested. For determining ω (the excitation frequency), we choose a characteristic time during which the strain changes considerably in experiments, and we identify this length of time with the half-period of a certain steady-state, dynamic action, the choice having been made at a location sufficiently remote from the composite rod's end-face, where any dynamic edge effect has vanished. Table 1 provides the estimate of ω for each experiment and the results of theoretical calculations and experiments. The following values were used in calculations: $\rho_c = 1.2$ g/cm^3 for the resin; $\rho_a = 7.8$ g/cm^3 for steel; $E_a = 2.1\cdot10^5$ MPa. Here, E_c is the elasticity modulus of the resin, χ is the volumetric percentage of steel in the composite rod, q_0 is the theoretical value of the edge effect for $a_{21} = a_{32}$, q_1 is the same, but with an allowance for the coefficients a_{21} and a_{32}, and q_* is the experimental value of the edge effect. The difference between the values of q_0 and q_1 increases with the coefficient a_{21}, which is determined by ν_2. With an increase in ν_2 from 0.03 to 0.25 in our calculations, the difference between q_0 and q_1 increases from 3 to 30%.

For clarity, the theoretical and experimental values of the edge effect are shown in Fig. 3, where 1 is the experimental value of q_*, 2 is the theoretical value of q_0, and 3 is the theoretical value of q_1 for $a_{21} \neq a_{32} \neq 0$.

Analysis of the results obtained indicates that, with an increase in the anisotropy parameter E_1/G, the zone of penetration of the edge effect increases, but the numerical values of q and q_* vary in both the experimental and the theoretical results. The experimental values of q_* exceed the theoretical values by a factor of 1.2-1.6.

Returning to the problem under consideration and a qualitative comparison between the theoretical calculations and experimental results, we should mention that this comparison is not quite correct. First, the load used in experiments was not taken into account in calculations. Second, the calculations were performed for two-dimensional strain, while axisymmetric loading was used in the experiments. In the third place, the proposed theory does not reflect the strongly pronounced structure of the specimens tested. However, there was a qualitative agreement between the proposed theory for determining the depth of penetration of the edge effect and the experimental results. The theoretical results and the experimental data both indicate that the zone of the edge effect increases with the anisotropy parameter E_1/G.

LITERATURE CITED

1. L. I. Slepyan, Transient Elastic Waves [in Russian], Leningrad (1972).
2. V. M. Kornev, "Refined theories of the extension and bending of orthotropic fittings," in: Dynamics of Continuous Media [in Russian], Vol. 51, Collection of Scientific Papers, Institute of Hydrodynamics, Siberian Branch, Academy of Sciences of the USSR (1982).
3. S. G. Lekhnitskii, Anisotropic Plates [in Russian], Moscow—Leningrad (1974).
4. A. G. Demeshkin and V. M. Kornev, "Propagation of strain pulses along composite rods," Mekh. Komposit. Mater., No. 1 (1984).
5. A. K. Malmeister, V. P. Tamuzh, and G. A. Teters, Strength of Rigid Polymer Materials [in Russian], Riga (1972).